Theory of Quantum Dots: An Introductory Review

D. Barzilay, H. Soifer.
Department of Physics, Tel Aviv University, Tel Aviv, Israel.

Quantum dots have penetrated our everyday life through their existing applications such as the QLED TVs, while also promising an exciting future with their solar energy, medical and military applications. This review examines the different theoretical approaches to understanding this technology. Specifically, we collect the results of early theoretical physics papers that derive from first principles the basic ideas and physical phenomenon governing QDs, explain them in detail, and compare their results with experimental evidence.

I. INTRODUCTION

In recent decades, the field of nanotechnology has witnessed remarkable advancement [1]. Reaching the nanometer scale (10^{-9} m) has enabled tinkering with the fundamental processes of light-matter interaction and the quantum behavior of matter. This unprecedented control comes to fruition in the development of novel materials with unique properties and exciting applications. Among these revolutionary materials, quantum dots have emerged as promising contenders due to their extraordinary electronic and optical characteristics. Quantum dots (QD), also called semiconductor nanocrystals, are nanoscale semiconductor particles, typically ranging from 1 to 100 nanometers in diameter, that exhibit their unique properties due to *quantum confinement* (described below). Unlike traditional bulk semiconductors, the physical size of a QD determines its bandgap (described below), which in turn determines its resonant wavelength for absorption and emission of light.

The most common type of QDs is called Colloidal quantum dots. They are obtained through chemical synthesis methods where the size and shape can be controlled by adjusting factors such as the reaction duration (see Figure 1), temperature, and the type of ligand molecules used. Colloidal quantum dots are typically spherical in shape and are often smaller than other synthesis methods, sometimes as tiny as 2-4 nm in diameter. [2,3]

This review begins with the modern motivation to understand QDs, which is based on their ground-breaking technology promises – as well as their current use in everyday consumer electronics. After which, a brief introduction to the elementary concepts needed to present the quantum dots is given, together with a short history of the discovery of QDs. Then, we'll review the theoretical approaches to modelling QDs properties with a focus on their size dependance, while showing in an organized fashion the derivation of a simple effective mass QD model.

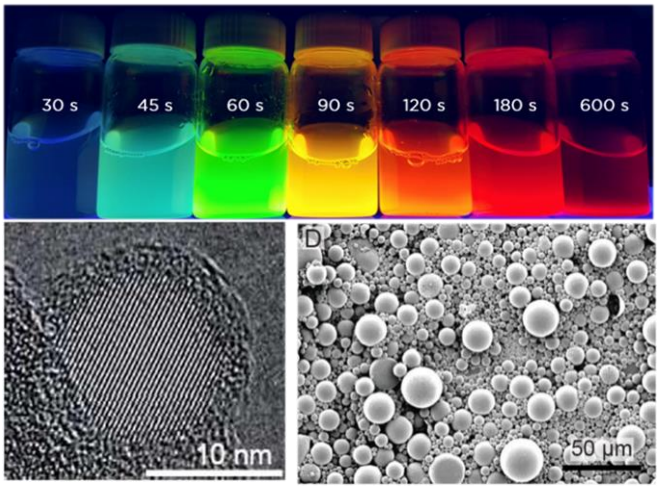

Figure 1. Top: Fluorescing QDs of different sizes. The longer the reaction time the bigger the colloidal QDs are, and the smaller the optical gap. [4] Left: TEM image of a Silicon QD. [5] Right: SEM image of PMMA microparticles containing $S_{10}C_5H$ QDs. [6]

A. Motivation - Applications

The possibility of using QDs for TV displays first appeared when their bandgaps were tuned to the entire visible range [7]. The first commercial QLED TV appeared in 2013 by Sony. The QLED TV working principle is to utilize light from a blue LED backlight that is converted by QDs fluorescence to relatively pure red and green, instead of the original concept of passing white light through color filters. This results in more precise colors and a large increase in brightness while using about 30 to 50 percent less power [8]. Newer QLED technologies ditch the blue backlight and use the QDs themselves as a light source using their photoexcitation by external current.

Since then, quantum dots are starting to be used in many other exciting applications. Less known, QDs have been used in the last ~10 years as a sensor for detection of explosives traces [9]. New generation solar cells achieve greater efficiency due to QDs ability to generate multiple excited electrons from a single photon [10]. Moreover, QDs small size allows to inject micro patches of them onto human skin to invisibly track population vaccination in developing countries [6].

QDs even take part in futuristic technologies such as quantum computing with a new research succeeding in demonstrating quantum interference of identical photons from *remote* GaAs QDs [11], as well as modern research in condensed-matter physics engineering a quantum simulation using topological states in QDs [12].

All this is ought to give enough motivation to understand the basic ideas around QD useful properties.

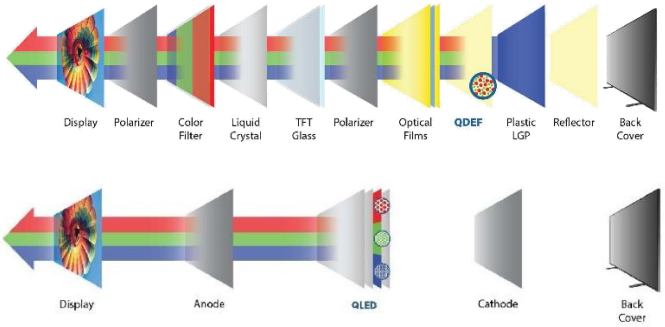

Figure 2. The operating principle of older (top) and newer (bottom) QLED TVs. [8]

B. Semiconductor-light interaction

Semiconductors are solid-state objects defined by their electric conductive behavior, somewhere between that of a conductor and an insulator. To understand how light interacts with the semiconductor it is necessary to look at the quantum states of the electrons in the material with which the light interacts. In a single atom, for example the Hydrogen, the electrons have atomic orbitals with discrete energy levels. When many such atoms are organized in a periodic lattice (as they do in semiconductor solids) the orbitals overlap to create energy *bands* – a continuous range of allowed energies [13]. In a semiconductor the bands are separated by a gap of forbidden energies called the *bandgap* E_g (see Figure 4). The lower energy band is called the *valance band,* which is where the electrons are found in their rest state. The higher energy band is called the *conduction band* because when an electron is excited to the conduction band it can gather momentum and participate in conducting a current.

Therefore, photons with energy larger than the bandgap (also called *optical gap* in this context) can be absorbed when interacting with a semiconductor by exciting an electron to the conduction band, an effect called *photoexcitation*. Once the electron is excited, it leaves behind what is a called a *hole* (the lack of an electron). The hole is a useful quasiparticle with positive-charge and positive-mass that simplifies calculating the dynamics of an almost-full valance band. When no external voltage is applied (called *bias*) to pull the electron and hole apart, they will recombine after a time called the *relaxation time*. On recombination they will emit a photon of their combined energy (an effect called *fluorescence*) and the system will return to its rest state (see the fluorescence at the top of Figure 1).

The hole and excited electron both have their own wavefunctions describing them and can simplistically be modelled as free particles with an effective mass (m_h^*, m_e^* respectively) [14]. It is important to mention that the excited electron and hole also interact by Coulomb attraction and may form bound states called *excitons* [15]. The individual wavefunctions of the hole and the electron, as well as the exciton binding energy, restricted under quantum confinement - will dictate the properties of the quantum dots.

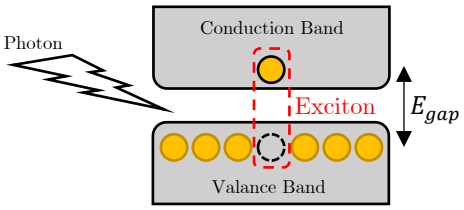

Figure 3. A photon excites an electron to the conduction band, leaving behind a hole. The hole and the electron are bound in a state called an Exciton.

C. Quantum confinement

Quantum confinement is the spatial restriction of a wavefunction in one or more dimensions within a material. In a bulk semiconductor, the physical size of the material is many orders of magnitude larger than the crystal lattice distances, so in practice it is treated extremely well as a lattice that spreads infinitely with no confinement (i.e., a 3-dimensional object with 0 dimensions of confinement). Very thin plates, whose thickness is near the scale of the lattice constants are called *quantum wells* which are 2-dimensional objects with 1 dimension of confinement (z direction). Likewise,

there are *nanowires* which are 1-dimensional and finally the quantum dots which are called 0-dimensional with 3 dimensions of confinement. The quantum effect of confinement is analogous to a particle in a box and forces the wavefunctions to vanish on the surfaces which usually causes discretization of energy levels, which gives confined materials such as the QDs their unique properties.

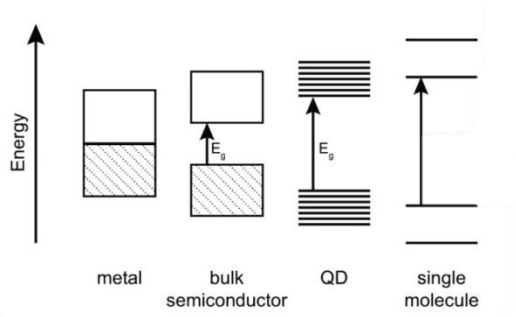

Figure 4. Energy states of electrons in different materials. Semiconductors have continuous bands of allowed energies. QDs have an extended optical gap due to confinement and single molecules have completely discrete energy levels. Adapted from [9].

D. History

The concept that the molecular and atomic discrete energy levels merge into continuous bands has been long understood in principle, but until the 80's it still wasn't observed experimentally. That is, discrete energy levels of molecules and atoms have been observed, as well as the continuous bands of many such atoms organized in a lattice – but never the transition point between them. Quantum dots are objects that are right at the tipping point between having molecular to solid-state electronic properties.[16]

QDs were first synthesized in 1981 by Soviet physicist Alexey Ekimov [17], followed by the first theoretical description in 1982 by Alexander Efros [18].

II. THEORETICAL APPROACHES

The goal of a theoretical description is to provide an explanation and/or predictions for a phenomenon of interest. In the case of quantum dots, many aspects can be analyzed – the chemical reactions to produce them, their atomic structure, their electronic and optical properties and so on. For different goals different theoretical approaches may be more appropriate. Practically, the simplest model that described experiments and predicts phenomena well is the first one to start with. For example, to get a pretty good approximation of the dependance of the optical gap on the dot's size, a simple time-independent single-particle approach that will shortly be described might be enough. In contrast, to visualize the inner structure of an excited quantum dot and to accurately predict the absorption spectrum, a very precise time-dependent multi-body model of the electrons wavefunctions is used (in [19] and Figure 5). These advanced models are disadvantageous in both complexity and computational cost – hence the reason to only use them when really needed.

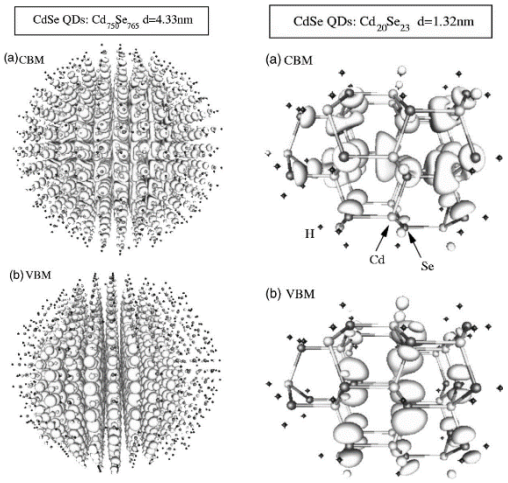

Figure 5. Example of an advanced theoretical model to predict QD structure. Lowest excited state (CBM) vs highest valance state (VBM) wavefunction isosurfaces (20% of maximum) in QDs. Left: 4.33nm QD. Right: 1.32nm QD. Simulated using density functional theory (DFT) under local density approximation (LDA) with self-consistent plane-wave pseudopotentials (PWP) method. Adapted from [19].

For this paper, we'd like a model that predicts the size at which an isotropic semiconductor sphere becomes a quantum dot, and the scaling law dependance of the optical gap on the QD size. The most basic model, described in full by Brus from Bell Labs [16], considers the excited electron (with effective mass m_e^*), the left-behind hole (m_h^*), and their coulomb interaction energy. We ignore an effect called dielectric confinement, as well as the exchange-interaction of the electron-hole spin as they were shown to be less significant for the size dependence in the *strong confinement* regime (defined later) [20].

The situation is then approximately described by a hydrogen-like Hamiltonian [15,16]:

$$(1)\quad \hat{H} = -\frac{\hbar^2}{2m_h^*}\nabla_h^2 - \frac{\hbar^2}{2m_e^*}\nabla_e^2 - \frac{e^2}{\epsilon|r_e - r_h|} + \textit{polarization terms}$$

where ϵ is the semiconductor permittivity (dielectric constant) which is dimensionless in CGS units. The polarization terms arise from induced charges on the

surfaces of the dot, caused by the change in dielectric constant – in analogy to electrostatic image charges. We shall apply a few approximations to solve this problem analytically.

A. Small polarization terms

The polarization terms can be written explicitly as:

$$P(\boldsymbol{r_e},\boldsymbol{r_e}) + P(\boldsymbol{r_h},\boldsymbol{r_h}) - P(\boldsymbol{r_e},\boldsymbol{r_h}) - P(\boldsymbol{r_h},\boldsymbol{r_e}) \tag{2}$$

where $P(\boldsymbol{r_i},\boldsymbol{r_j})$ are the interaction potentials of the charge at $\boldsymbol{r_i}$ (electron or hole) with the surface-induced image charge caused by the charge at $\boldsymbol{r_j}$ (for explicit expression see Appendix A). Because of the small size of the quantum dot, the hole and the electron are closely localized such that $\boldsymbol{r_e}\sim\boldsymbol{r_h}$, which causes the polarization terms to be very small relative to the other terms in the Hamiltonian and ignored in practice for spherical QDs. [21].

B. Confinement regimes

Further simplification is needed to solve the problem analytically. As of now, the Hamiltonian without any boundary conditions describes a free exciton, which is a two-body problem that can be solved as if it was a one-body problem (exactly like the hydrogen problem!) using the reduced mass of the electron and hole.

On the other hand, ignoring the coulomb interaction leaves us with a simple "particle in a sphere" problem that is also analytically solvable to give discrete energy levels dependent on the size of the sphere, as we'll see later on.

As our interest is in the size dependance of the QD, we'd like a way to identify the regime at which the coulomb interaction is less important than the size constraints, so it can be treated as a perturbation within good approximation. The rigorous approach to do so is to compare the effect's energy scales, but it turns out in this case that comparing each effect length scale gives about the same result (see Appendix B).

Returning to the unbounded exciton which is solvable like the hydrogen atom, the resulting exciton wavefunction has a size characterized by the relevant Bohr radius $a_B^* = \frac{\epsilon}{\mu/m_e} a_0$ where in CGS units ϵ is the QD dielectric constant, m_e is the standard electron mass, $a_0 = \frac{\hbar^2}{e^2 m_e}$ is the standard Bohr radius, and $\mu \equiv \frac{m_e^* m_h^*}{m_e^* + m_h^*}$ is the reduced mass. [15]

The excitonic Bohr radius a_B^* defines the length scale that allows identifying three regimes by comparing it to the QD radius R:

Weak confinement regime is where $a_B^* \ll R$, so the electron and hole won't be affected by the potential barriers of the surfaces, as they are much further away than their wavefunctions spread. This is the case with the regular bulk semiconductor (i.e., This is not a QD!)

Intermediate confinement is where $a_B^* \approx R$, a more complicated regime that requires the equal treatment of the coulomb interaction and the discretization due to the QD boundaries. This is the relevant scale at which semiconductors start to behave like QDs!

Strong confinement regime is where $a_B^* \gg R$, in which the confinement by the potential barriers at the surfaces have greater significance then the coulomb interaction. This is the regime of our interest, in which we'll treat the coulomb interaction as a perturbation to the free electron and hole confined in a sphere.

To get things into perspective, the Bohr exciton radius is usually in the range of 1~10 nm, for example it is 3 nm for CdS, 4.3 nm for Silicon and 5.3 nm for CdSe with extreme cases like 0.75 nm for CuCl and 65.6 nm for InSb. Crystals manufactured at radiuses less than those will behave as QDs. [10,22]

C. Particle in a sphere

Focusing on the strong confinement regime, which is relevant for small QDs, we can treat the coulomb interaction as a small perturbation and begin by solving for the unperturbed case. Only the first two terms remain in the Hamiltonian from (1) which now describe a free electron and hole. Now that there is no interaction between the electron and hole, they can be solved separately, and the total energy will be the sum of the energy of them both. Enforcing an infinite potential barrier at the surfaces of the QD sphere (of radius R) – we get the boundary condition that the resulting wavefunctions should vanish on $|\boldsymbol{r}| = R$. This problem is easily solved very much like the foundational 1D particle in a box problem to give in spherical coordinates [18,20]:

$$\phi_{nlm}(\boldsymbol{r}) = A_{nl} \cdot j_l\left(z_{l,n} \cdot \frac{r}{R}\right) Y_{lm}(\theta,\varphi) \tag{3}$$

$$E_{n,l} = \frac{\hbar^2}{2mR^2} z_{l,n}^2 \tag{4}$$

where Y_{lm} are the spherical harmonics giving rise to the quantum numbers l, m. A_{nl} is a normalization constant and $z_{l,n}$ is the nth zero of the spherical Bessel function

j_l (i.e., $j_l(z_{l,n}) = 0$) which is an increasing function of both n and l.

The dependance on the natural number n arising from quantum confinement is the representation of the energy discretization of QDs. Focusing on the lowest energy state of our excited system, $l = 0, n = 1$, the wavefunctions become of the form:

$$\phi_0(\boldsymbol{r}) = \frac{1}{\sqrt{2\pi R}} \cdot \frac{sin\left(\pi \cdot \frac{r}{R}\right)}{r} \tag{5}$$

the complete wavefunction for the electron and hole is:

$$\psi_0(\boldsymbol{r_e}, \boldsymbol{r_h}) = \phi_0(\boldsymbol{r_e}) \cdot \phi_0(\boldsymbol{r_h}) \tag{6}$$

and the energy:

$$E_0 = \frac{\pi^2\hbar^2}{2R^2}\left(\frac{1}{m_e^*} + \frac{1}{m_h^*}\right) = \frac{\pi^2\hbar^2}{2\mu R^2} = \frac{\pi^2}{2} \cdot \frac{e^4\mu}{\epsilon^2\hbar^2} \cdot \left(\frac{a_B^*}{R}\right)^2 \tag{7}$$

where, as defined above, μ is the reduced mass and a_B^* is the exciton Bohr radius. Switching the masses to μ clarifies the interpretation of a single exciton in a sphere.

D. Including the Coulomb interaction

In the strong confinement regime approximation, the coulomb interaction can be treated as a small perturbation. Two equivalent ways to think about adding it are either as a perturbation theory first-order correction to (7) or by using the variational method with ψ_0 from (6) as the trial function (without minimization). As promised by the variational method, this will give an upper bound on the ground state energy of our excited system. Both approaches result in the matrix element:

$$\Delta E_0 = \langle\psi_0| \frac{-e^2}{\epsilon|\boldsymbol{r_e} - \boldsymbol{r_h}|} |\psi_0\rangle = \tag{8}$$

$$\frac{-e^2}{\epsilon\pi R^2} \int d\Omega \int_0^R dr_e \int_0^R dr_h \frac{sin^2\left(\pi \cdot \frac{r_e}{R}\right) sin^2\left(\pi \cdot \frac{r_h}{R}\right)}{(r_e r_h)^2} \frac{r_e^2 r_h^2}{\sqrt{r_e^2 + r_h^2 - 2r_e r_h cos\theta}}$$

which can be calculated (see Appendix C) to give:

$$\Delta E_0 = -A\frac{e^2}{\epsilon R} = -A\frac{e^4\mu}{\epsilon^2\hbar^2} \cdot \left(\frac{a_B^*}{R}\right) \tag{9}$$

where $A = 2 - \frac{\mathrm{Si}(2\pi)}{\pi} + \frac{\mathrm{Si}(4\pi)}{2\pi} \approx 1.786$ and Si(x) is the *sine integral function*. As defined above, μ is the reduced mass and a_B^* is the exciton Bohr radius.

It's important to note that this result is self-consistent with the assumption that in the strong confinement regime ($\lambda = \frac{a_B^*}{R} \gg 1$) the energy from quantum confinement (7) is more significant ($\propto \lambda^2$) than the energy from the coulomb interaction ($\propto \lambda$).

E. Size dependance

Collecting all the result so far, the lowest energy of the system after photoexcitation with respect to the rest state can written:

$$E_0 = E_{gap} + \frac{e^4\mu}{\epsilon^2\hbar^2}\left[\frac{\pi^2}{2}\left(\frac{a_B^*}{R}\right)^2 - 1.786\left(\frac{a_B^*}{R}\right)\right] \tag{10}$$

where E_{gap} is the bulk semiconductor bandgap.

Even though this derivation was made with simplifying assumption, the result implies that as the size of the quantum dot gets smaller, the effective optical gap E_0 gets larger and the photons absorbed and emitted will be of a shorter wavelength, which was verified experimentally [23]. Furthermore, as the radius of the QD gets larger, and the semiconductor reaches its weak confinement regime in which it acts as a normal bulk semiconductor, the extra terms vanish, which gives $\frac{a_B^*}{R} \to 0 : E_0 \to E_{gap}$ as expected.

Unfortunately, as can be seen in both Figure 6 and Figure 7, when looking to get an exact prediction for the energy $E(R)$, this model deviates from measurements. Its shortcoming gave rise to more elaborate approaches such as the successful *pseudo-potential* method that is beyond the scope of this introductory review.

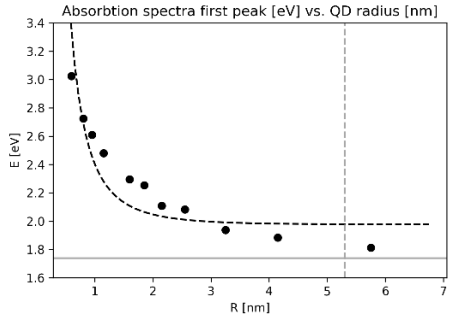

Figure 6. Dashed curve: Our fit of Eq. 10 to measurements of CdSe QDs from [23]. In solid gray is the bulk CdSe bandgap at $E_g = 1.74\ eV$, in dashed its exciton Bohr radius $a_B^* = 5.3\ nm$.

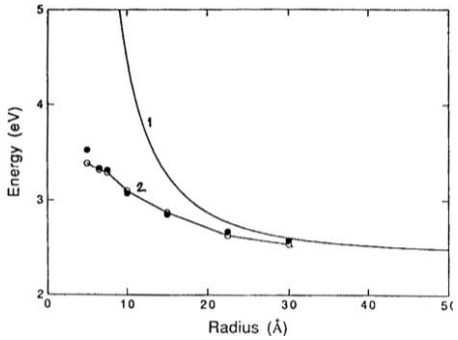

Figure 7. Absorption energies (•) for CdS QDs ($E_g = 2.42eV$). 1: calculations using the model from Eq. (10); (o): pseudo-potential method calculations. Taken from [22].

III. OUTLOOK

In this paper, we explored the basic effective mass model to get a grasp of how quantum dots properties depend on their size, an effect that arises due to quantum confinement. We also mentioned a few more advanced theoretical approaches that allow a more precise calculation of QD properties such as their entire energy spectra, and their dependence on shape.

Now, after establishing an elementary understanding of quantum dots applications and theoretical working principles, their historical intertwined development can be appreciated and looked upon as indicative to the future.

Even through a very basic theoretical understanding of this disruptive nanoscale material, widespread devices such as QLED TVs have been possible to envision and develop, as well as the described emerging technologies in various fields. We think that the continued development of more advanced and precise theoretical models will play a pivotal role in discovering and controlling QDs properties, thus enabling new applications that will propel the quantum dot technology to new heights.

[1] H.N. Cheng, L.J. Doemeny, C.L. Geraci, D. Grob Schmidt, Nanotechnology Overview: Opportunities and Challenges, in: Nanotechnology: Delivering on the Promise Volume 1, American Chemical Society, 2016: pp. 1–12. https://doi.org/10.1021/bk-2016-1220.ch001.

[2] A.P. Alivisatos, Semiconductor Clusters, Nanocrystals, and Quantum Dots, Science. 271 (1996) 933–937. https://doi.org/10.1126/science.271.5251.933.

[3] X. Michalet, F.F. Pinaud, L.A. Bentolila, J.M. Tsay, S. Doose, J.J. Li, G. Sundaresan, A.M. Wu, S.S. Gambhir, S. Weiss, Quantum dots for live cells, in vivo imaging, and diagnostics, Science. 307 (2005) 538–544. https://doi.org/10.1126/science.1104274.

[4] Quantum dots: Harnessing the nanoscopic rainbow, Chem 13 News Magazine. (2018). https://uwaterloo.ca/chem13-news-magazine/november-2017/feature/quantum-dots-harnessing-nanoscopic-rainbow (accessed May 16, 2023).

[5] D. Hippo, H.-J. Chong, Y. Kawata, A. Tanaka, Y. Tsuchiya, H. Miwta, S. Oda, K. Urakawa, N. Koshida, A new design of nanocrystalline silicon optical devices based on 3-dimensional photonic crystal structures, in: 2005: pp. 114–116. https://doi.org/10.1109/GROUP4.2005.1516422.

[6] K.J. McHugh, L. Jing, S.Y. Severt, M. Cruz, M. Sarmadi, H.S.N. Jayawardena, C.F. Perkinson, F. Larusson, S. Rose, S. Tomasic, T. Graf, S.Y. Tzeng, J.L. Sugarman, D. Vlasic, M. Peters, N. Peterson, L. Wood, W. Tang, J. Yeom, J. Collins, P.A. Welkhoff, A. Karchin, M. Tse, M. Gao, M.G. Bawendi, R. Langer, A. Jaklenec, Biocompatible near-infrared quantum dots delivered to the skin by microneedle patches record vaccination, Science Translational Medicine. 11 (2019) eaay7162. https://doi.org/10.1126/scitranslmed.aay7162.

[7] P.O. Anikeeva, J.E. Halpert, M.G. Bawendi, V. Bulović, Quantum Dot Light-Emitting Devices with Electroluminescence Tunable over the Entire Visible Spectrum, Nano Lett. 9 (2009) 2532–2536. https://doi.org/10.1021/nl9002969.

[8] QUANTUM DOTS DISPLAY-QUANTUM DOTS DISPLAY-Suzhou Xingshuo Nanotech Co. Ltd., (n.d.). https://www.mesolight.com/QUANTUMDOTSDISPLAY/28.html (accessed May 21, 2023).

[9] W.J. Peveler, S.B. Jaber, I.P. Parkin, Nanoparticles in explosives detection – the state-of-the-art and future directions, Forensic Sci Med Pathol. 13 (2017) 490–494. https://doi.org/10.1007/s12024-017-9903-4.

[10] P. Bhambhani, Quantum Dot-sensitized Solar Cells: A Review, Bulletin of Electrical Engineering and Informatics. 7 (2018) 42–54. https://doi.org/10.11591/eei.v7i1.841.

[11] L. Zhai, G.N. Nguyen, C. Spinnler, J. Ritzmann, M.C. Löbl, A.D. Wieck, A. Ludwig, A. Javadi, R.J. Warburton, Quantum interference of identical photons from remote GaAs quantum dots, Nat. Nanotechnol. 17 (2022) 829–833. https://doi.org/10.1038/s41565-022-01131-2.

[12] M. Kiczynski, S.K. Gorman, H. Geng, M.B. Donnelly, Y. Chung, Y. He, J.G. Keizer, M.Y. Simmons, Engineering topological states in atom-based semiconductor quantum dots, Nature. 606 (2022) 694–699. https://doi.org/10.1038/s41586-022-04706-0.

[13] S.A. Holgate, Understanding Solid State Physics, CRC Press, 2009.

[14] C. Kittel, Introduction to solid state physics, 8th ed, Wiley, Hoboken, N.J., 2005.

[15] K. Cho, ed., Excitons, Springer, Berlin, Heidelberg, 1979. https://doi.org/10.1007/978-3-642-81368-9.

[16] L. Brus, Electronic wave functions in semiconductor clusters: experiment and theory, J. Phys. Chem. 90 (1986) 2555–2560. https://doi.org/10.1021/j100403a003.

[17] A.I. Ekimov, Al.L. Efros, A.A. Onushchenko, Quantum size effect in semiconductor microcrystals, Solid State Communications. 56 (1985) 921–924. https://doi.org/10.1016/S0038-1098(85)80025-9.

[18] A. Efros, A. Efros, Interband Light Absorption in Semiconductor Spheres, Soviet Physics. Semiconductors. 16 (1982) 772–775.

[19] J. Li, L.-W. Wang, Band-structure-corrected local density approximation study of semiconductor quantum dots and wires, Phys. Rev. B. 72 (2005) 125325. https://doi.org/10.1103/PhysRevB.72.125325.

[20] T. Takagahara, Effects of dielectric confinement and electron-hole exchange interaction on excitonic states in semiconductor quantum dots, Phys. Rev. B. 47 (1993) 4569–4584. https://doi.org/10.1103/PhysRevB.47.4569.

[21] N. Vukmirovic, Quantum Dots: Theory, (2010). https://escholarship.org/uc/item/9mx648vg (accessed May 16, 2023).

[22] A.D. Yoffe, Low-dimensional systems: quantum size effects and electronic properties of semiconductor microcrystallites (zero-dimensional systems) and some quasi-two-dimensional systems, Advances in Physics. 42 (1993) 173–262. https://doi.org/10.1080/00018739300101484.

[23] C.B. Murray, D.J. Norris, M.G. Bawendi, Synthesis and characterization of nearly monodisperse CdE (E = sulfur, selenium, tellurium) semiconductor nanocrystallites, Journal of the American Chemical Society. (1993). https://doi.org/10.1021/ja00072a025.

APPENDIX A: POLARIZATION TERMS

The polarization terms are given specifically by the classical treatments of two charges in a dielectric sphere:

$$P(r_1, r_2) = \frac{e^2}{R}\sum_{n=0}^{\infty} \alpha_n \left(\frac{r_1 r_2}{R^2}\right)^n P_n(\cos\theta_{12})$$

where $\alpha_n = \frac{(n+1)(\epsilon-1)}{\epsilon(n\epsilon+n+1)}$, P_n is the Legendre polynomial, θ_{12} is the angle between $\boldsymbol{r_1}$ and $\boldsymbol{r_2}$. As the electron and hole have the exact opposite charge, in the limit where $\boldsymbol{r_e} = \boldsymbol{r_h}$, the polarization terms cancel out to zero exactly.

APPENDIX B: CONFINEMENT REGIMES

Perturbation theory is correctly applied when the perturbation energy is much smaller than the difference between unperturbed energy levels. The difference between the first and second excited states of an unperturbed particle in a sphere according to Eq. (4) is:

$$D = \frac{\hbar^2}{2\mu R^2}(z_{11}^2 - z_{01}^2) = \frac{\hbar^2}{2\mu R^2}\cdot((4.49)^2 - (3.14)^2) \approx \frac{10.3\cdot\hbar^2}{2\mu R^2}$$

where μ is the reduced mass. The energy of the perturbation is the lowest $n = 1$ energy of the hydrogen-like exciton: $E_{c,0} = -\frac{\hbar^2}{2\mu(a_B^*)^2}$. So, the comparison is then:

$$|E_{c,0}| \ll |D| \quad which\ yields \quad \left(\frac{R}{a_B^*}\right) \ll \sqrt{10.3} \approx 3.2$$

which is in the order of magnitude of 1 so it is good enough to compare the radius for a good measure of the relevant regime.

APPENDIX C: MATRIX ELEMENT CALCULATION

$$\psi_0 = \frac{1}{2\pi R}\cdot\frac{sin\left(\pi\cdot\frac{r_e}{R}\right)}{r_e}\cdot\frac{sin\left(\pi\cdot\frac{r_h}{R}\right)}{r_h}$$

$$\Delta E_0 = \langle\psi_0|\frac{-e^2}{\epsilon|\boldsymbol{r_e} - \boldsymbol{r_h}|}|\psi_0\rangle$$

$$= \frac{-e^2}{\epsilon(2\pi R)^2}\int_0^R dr_e\int_0^R dr_h \frac{sin^2\left(\pi\cdot\frac{r_e}{R}\right)sin^2\left(\pi\cdot\frac{r_h}{R}\right)}{(r_e r_h)^2}\int d\Omega_h\int d\Omega_e \frac{r_e^2 r_h^2}{\sqrt{r_e^2 + r_h^2 - 2r_e r_h cos\theta_{eh}}}$$

where θ_{eh} is the angle between $\boldsymbol{r_e}$ and $\boldsymbol{r_h}$. Because of the spherical symmetry, we can simplify by choosing $\boldsymbol{z}||\boldsymbol{r_e}$ such that $\theta_{eh} = \theta_h \equiv \theta$ so can compute $\int d\Omega_e = 4\pi$:

$$= \frac{-e^2}{\epsilon\pi R^2}\int_0^R dr_e\int_0^R dr_h \frac{sin^2\left(\pi\cdot\frac{r_e}{R}\right)sin^2\left(\pi\cdot\frac{r_h}{R}\right)}{(r_e r_h)^2}\int d\Omega \frac{r_e^2 r_h^2}{\sqrt{r_e^2 + r_h^2 - 2r_e r_h cos\theta}}$$

Canceling terms and preparing the $d\Omega$ integral:

$$= \frac{-e^2}{\epsilon\pi R^2}\int_0^R dr_e\int_0^R dr_h\, sin^2\left(\frac{\pi r_e}{R}\right)sin^2\left(\frac{\pi r_h}{R}\right)\int d\phi d(cos\,\theta) \cdot \frac{1}{\sqrt{r_e^2 + r_h^2 - 2r_e r_h cos\theta}}$$

Doing the angular integrals:

$$= \frac{-e^2}{\epsilon\pi R^2}\int_0^R dr_e\int_0^R dr_h\, sin^2\left(\frac{\pi r_e}{R}\right)sin^2\left(\frac{\pi r_h}{R}\right) \cdot 2\pi\left[-\frac{2}{2r_h r_e}\sqrt{r_e^2 + r_h^2 - 2r_e r_h\, cos\,\theta}\right]_{-1}^{1}$$

$$= \frac{-2e^2}{\epsilon R^2}\int_0^R dr_e\int_0^R dr_h\, sin^2\left(\frac{\pi r_e}{R}\right)sin^2\left(\frac{\pi r_h}{R}\right)\cdot\frac{|r_e + r_h| - |r_e - r_h|}{r_h r_e}$$

Because of the symmetry between r_e and r_h in the integral, we calculate it for $r_h < r_e$ and double the result:

$$= \frac{-4e^2}{\epsilon R^2}\int_0^R dr_e\int_0^{r_e} dr_h\, sin^2\left(\frac{\pi r_e}{R}\right)sin^2\left(\frac{\pi r_h}{R}\right)\cdot\frac{r_e + r_h - r_e + r_h}{r_h r_e} =$$

$$= \frac{-4e^2}{\epsilon R^2}\int_0^R dr_e\int_0^{r_e} dr_h\, sin^2\left(\frac{\pi r_e}{R}\right)sin^2\left(\frac{\pi r_h}{R}\right)\cdot\frac{2}{r_e} =$$

$$= \frac{-8e^2}{\epsilon R^2}\int_0^R dr_e\frac{sin^2\left(\frac{\pi r_e}{R}\right)}{r_e}\int_0^{r_e} dr_h\, sin^2\left(\frac{\pi r_h}{R}\right)$$

Doing the dr_h integral:

$$= \frac{-8e^2}{\epsilon R^2}\int_0^R dr_e\frac{sin^2\left(\frac{\pi r_e}{R}\right)}{r_e}\left[\frac{r_e}{2} - \frac{R\sin\left(\frac{2\pi r_e}{R}\right)}{4\pi}\right]$$

Finishing with the dr_e integral:

$$= \frac{-8e^2}{\epsilon R^2}\cdot\left[R\cdot\frac{4\pi - 2Si(2\pi) + Si(4\pi)}{16\pi}\right] = \frac{-e^2}{\epsilon R}\left[2 - \frac{Si(2\pi)}{\pi} + \frac{Si(4\pi)}{2\pi}\right]$$

$$\approx -1.786\cdot\frac{e^2}{\epsilon R}$$

where $Si(x)$ is the sine integral function.